Decision Science Letters 15 (2026) 1399–1416

Contents lists available at GrowingScience

Decision Science Letters

homepage: www.GrowingScience.com/dsl

A stochastic simulation framework for long-term dead sea level forecasting under RSDS inflow scenarios with stability-aware dynamics

Afaf Edinat[a*], Tamara Baker Jber[a], Mariam Al Ghamri[a], Fatima Haimour[b], Mohammad Shehab[a], Bashar S. Khassawneh[a] and Hanaa Fathi[a]

[a]*College of Information Technology, Amman Arab University, Amman 11953, Jordan*
[b]*Faculty of Information Technology, Zarqa University, Jordan*

C H R O N I C L E

Article history:
Received April 3 2026
Received in Revised Format May 29 2026
Accepted June 22 2026
Available online June 22 2026

Keywords:
Dead Sea
Model and Simulation
Predict levels of Dead Sea
Red-Dead Sea (RSDS) Project
Water Conveyance
Water levels of Dead Sea
Water volumes of Dead Sea
Energy

A B S T R A C T

The continuous decline of the Dead Sea water level represents one of the most critical environmental challenges in the Middle East, primarily caused by reduced inflow from the Jordan River basin and increased regional water consumption. Predicting the long-term evolution of the Dead Sea is therefore essential for evaluating the potential effectiveness of large-scale restoration initiatives such as the Red Sea--Dead Sea (RSDS) conveyance project. In this study, a stochastic simulation framework is proposed to model and predict the long-term dynamics of the Dead Sea water level under multiple inflow scenarios. The framework integrates probabilistic increment generation, recursive hydrological updating, and stability-aware monitoring within a unified computational procedure. Annual water-level increments are generated using statistically fitted probability distributions derived from historical observations, enabling the model to capture the inherent variability and uncertainty of natural hydrological processes. The system state is iteratively updated across the simulation horizon, while a stability index is used to evaluate convergence behavior and detect potential equilibrium conditions. Five representative RSDS scenarios are investigated, including baseline recovery, moderate inflow, accelerated recharge, threshold-stabilized inflow, and high-variability environmental conditions. Simulation results indicate that under the baseline scenario the Dead Sea level increases gradually from approximately −434 m to about −60 m within 500 simulation steps, whereas accelerated recharge conditions can raise the level beyond 200 m due to higher early-stage inflow rates. The threshold-stabilized scenario reveals regime transitions in increment dynamics that lead to a near-equilibrium state, while the high-variability scenario exhibits strong stochastic fluctuations with annual increments ranging between 0.4 and 2.2 m. Overall, the results demonstrate that the proposed framework effectively captures diverse hydrological behaviors and provides a flexible and computationally efficient tool for long-term forecasting and policy evaluation of Dead Sea restoration strategies.

© 2026 by the authors; licensee Growing Science, Canada

1. Introduction

The Dead Sea is located within the Jordan Rift Valley, which stretches over 400 km from Lake Tiberias in the north to the Gulf of Aqaba in the south. This region includes the Jordan River Valley, the Dead Sea, and Wadi Araba. The Dead Sea now covers an area of 1,001 km², is 79.5 km long, and has a maximum width of 17.5 km. It is a terminal lake that consists of two distinct parts, almost separated by the Lisan Peninsula, which is just out from its eastern shore. The southern part is 244 km² large and quite shallow; it rarely exceeds the depth of 10 m. By contrast, the basin north of the Lisan Peninsula measures 757 km² and is 400 m deep in its eastern part. The volume of the Dead Sea is about 143 km³ (Yousef, 2025; Bzour et al., 2025). Situated at the lowest point on Earth, the Dead Sea is an extraordinary site, renowned for its outstanding geological phenomena, long history, and crucial ecological function, turning it into one of natural wonders. This exceptional tourism destination attracts millions each year. Yet, despite its natural beauty and biodiversity value, the Dead Sea is suffering from a serious environmental problem: in the last few decades, its water level has dropped more than one meter annually. The main cause for the drop is human intervention: diversion of water from the River Jordan and its system of tributaries, alongside

* Corresponding author
E-mail a.edinat@aau.edu.jo (A. Edinat)
ISSN 1929-5812 (Online) - ISSN 1929-5804 (Print)
2026 Growing Science Ltd.
doi: 10.5267/j.dsl.2026.6.013

considerable mineral extraction from its shoreline. Since the 1960s, its level has decreased by over 30 meters, and along its shores, it has created over 6,000 sinkholes (Baer et al., 2024). These vents threaten the local ecosystem, even causing infrastructural disruptions and losses in tourism. Fig. 1 presents the sources of freshwater that feed the Dead Sea.

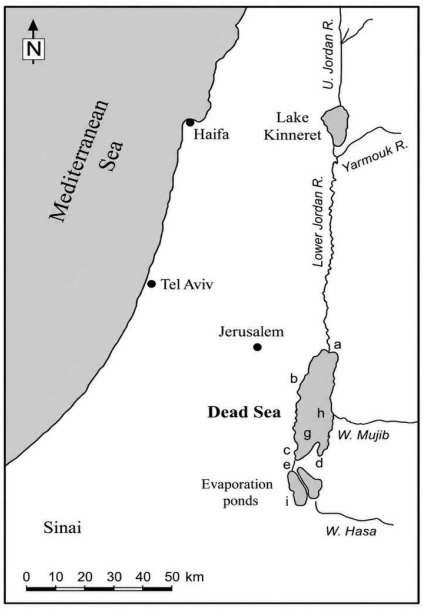

Fig. 1. Location map. Key freshwater sources: Jordan River (a), En Fesh'ha springs (b), Arnon- Mujib (c). Brine from the Dead Sea is pumped from point d to evaporation ponds, with concentrated brine redirected back to the Dead Sea at point e. Meteorological and hydrographic stations are at EG100 (g) and EG320 (h). Sedom (i) is within the evaporation pond (Lensky et al., 2005; Asad Ahmad, 2026).

Regional authorities are cooperating on an ambitious 180-km scheme to transport water from the Red Sea at Aqaba to the Dead Sea to stem its shrinkage (Al-Bakri et al., 2026). The scheme, called the Red-Dead project or the Red Sea Dead Sea Water Conveyance (RSDS), proposes to use a 400-meter drop in elevation to produce hydroelectricity, desalinate part of the water, and dispose of the brine waste in the Dead Sea to contribute to the restoration of its water level. Also under the scheme, desalted water will be lifted 1,000 meters for delivery to key urban areas in Jordan and, eventually maybe, in Palestine and neighbouring territories (Zawahri & Weinthal, 2025; Lensky et al., 2005). The concept of the Red Sea-Dead Sea (RSDS) was initially considered in the mid-1800s by British military personnel seeking alternatives to the Suez Canal, which the French had just built. This was done without the realization that the Dead Sea is hundreds of meters below sea level. In the late 1800s, there became a scientific interest in harnessing Jordan River water for irrigation and letting seawater into the Dead Sea to produce energy from an elevation difference of approximately 390 m below mean sea level (Wikipedia, 2023b; Wikipedia, 2023a). A canal between the Red Sea and Dead Sea was first envisioned in the late 1960s, when Jordan and the neighbouring states were discussing diplomatic relations. In the 1990s, a scheme was suggested for the development of the project in steps so the environmental impact of combining the two waters could be assessed in parts while minimizing the financial risk. Logistical issues, along with considerations of cost, led to the proposed development of the canal within Jordan. In 2005, Jordan and the neighbouring countries signed an agreement to begin a feasibility study for the "Two Seas Canal." In 2009, Jordan announced its decision to proceed unilaterally to develop the Jordan Red Sea Project (JRSP) and referred to it as the first phase of the RSDS. In 2016, the Jordanian government had shortlisted five consortiums that would move forward with the project (Bentor, 1961; Sommer & Fassbender, 2024; Wikipedia, 2023b).

The proposed conveyance system will pump seawater 230 meters uphill from the Gulf of Aqaba in the Red Sea through the Arabah Valley in Jordan. From this point, the water would flow gravitationally through various pipelines down to the area of the Dead Sea. After that, it would fall through a penstock down to the Dead Sea shoreline, about 420 meters below sea level, and then an open canal to the Sea itself. The project involves the construction of approximately 225 km of pipelines that can transport both seawater and brine, running parallel to the Arabah Valley, with around 178 km of pipes distributing freshwater to the Amman area. Core infrastructure facilities will include several stations for desalination and at least one hydroelectric station. It is expected that 850 million cubic meters of drinking water will be delivered by the project every year in its fully operational mode. The system will utilize the electricity grid of Jordan, while a part of the energy input it needs is produced as hydropower. However, the project is expected to be a net consumer of electricity, with more energy consumption than production. This additional requirement for energy has to be met by other sources of power, for which the cost lies outside the project budget (Wikipedia, 2023b; Wikipedia, 2023a). The specific purpose of this study is to develop a simulation model that can project future fluctuations in the Dead Sea water level. The model will estimate the rise in water level over the next

couple of years. A secondary objective is to simulate the water level stabilization based on the regulation of water intake from the Dead Sea Canal (RDSC).

2. Related Work

Bzour et al. (2025) evaluated the Red Sea-Dead Sea (Red-Dead) project in conjunction with other alternatives for the restoration of the Dead Sea's water levels. By making use of a hydro-economic model that links Jordan and other neighbouring lands, the analysis revealed that two alternatives to the proposed Red-Dead canal could realize higher cost efficiency. Pursuing a mix of decentralized strategies, developing additional sources of water, expanding wastewater reuse, strengthening infrastructure for better transport efficiency, promoting water conservation, and reducing leakage within the system, would result in improved overall economic efficiency and ensure an annual delivery of up to 900 million cubic meters (MCM) of water to the Dead Sea in these countries. A downscaled version of the Red-Dead project may also bring significant water inflow, provided that electricity produced could be sold at a price that could yield reasonable margins. Shekar and Mathew (2024) gave an in-depth analysis of geomorphological dynamics, an extensive array of processes that include soil erosion, channel deepening, degradation of the land surface, and collapse sinkholes. High-resolution airborne laser scanning was used to record topographic data in three dimensions over large areas, allowing exact measurements of volume changes and documentation of the present landscape with precision. Their findings are crucial in understanding how to foresee and plan for the future in such rapidly changing environments.

Salameh and El-Naser (2008) examined the pros and cons of the Red-Dead Canal project. They highlighted the fact that serious risk assessments would be required to mitigate the adverse impacts, which may include chemical interactions between various water sources, the deposition or dissolution of minerals, and environmental impacts related to the intake and Alignment locations proposed for the canal. Moreover, there are question marks over the structural soundness of the canal in the event of natural hazards such as earthquakes and floods. These factors also need to be researched in detail before construction commences (Al-Makhadmah et al., 2020). Lensky et al. (2005) conducted a quantitative assessment of energy and mass exchanges within the Dead Sea by using the meteorological and hydrographic observations gathered between 1996 and 2001. The calculations also looked at the impact of declining surface water inflow on the rate of evaporation in the region. Ghazleha et al. (2010) developed a mathematical model to calculate the volume of water in the Dead Sea within an elevation ranging from -390 to -415 meters above mean sea level. The model serves as an important tool that helps in predicting future volume variations with respect to alteration in water level. Abu-Faraj and Ghatasheh (as cited in Asmar, 2003) applied digital image processing methodologies to analyze the Dead Sea's water level decline. The emphasis in their research was on the use and interpretation of image-based methodologies, rather than the derivation of detailed predictions. In contrast, the current study utilizes actual measurements of the Dead Sea's level in conjunction with simulation tools that offer predictive capabilities for future trends (Al Hasanat et al., 2025). Alqadi and Kumar (2014) explored various traditional and modern methods of water management, focusing on systemic failures and providing recommendations on policy adjustment and infrastructure development. Their study emphasizes the immediate necessity of desalination plants, especially as part of a long-term solution to Jordan's growing domestic water demand. They also cite ineffective enforcement and lack of proper implementation of existing laws as major factors causing the continuous deterioration in the water situation.

3. Methodology

The initial phase of this study is the detailed definition of the system, which is essential for identifying the significant problems, specifically the expected increase in the water level of the Dead Sea and the energy production targets for the Red Sea-Dead Sea (RSDS) project. This is then followed by the statement of the main objectives of the study, after which the identification of the specific problems to be analysed will be clearly stated. The next section consists of the actual construction of the simulation model, to be followed by verification and validation to determine the model's reliability and efficiency. In the final sections, this study will present the interpretation and evaluation of the simulation results, from which conclusions will be made based on the analysed data. The methodological workflow illustrated in Fig. 2 represents a complete analytical pipeline used to evaluate the future hydrological behavior of the Dead Sea under the Red Sea--Dead Sea conveyance (RSDS) project scenario. The process begins with the collection of historical and projected Dead Sea level observations, which constitute the empirical basis for modeling the system dynamics. These observations are first transformed into annual level differences in order to capture the temporal evolution of the basin in a discrete form suitable for simulation. The resulting increments were then statistically analyzed using the Arena Input Analyzer to determine the appropriate probabilistic distribution that describes the variability of yearly level changes. This statistical characterization enables the modeling framework to incorporate the stochastic nature of environmental processes rather than relying solely on deterministic assumptions. Once the distribution parameters were identified, they are integrated into the water-level prediction module, where the recursive relationship between successive yearly levels were iteratively evaluated to simulate the long-term trajectory of the Dead Sea elevation. After the water-level evolution has been generated through the simulation process, the framework proceeds to the second analytical stage in which predicted elevation values are translated into corresponding water volumes using the elevation--volume relationship. This transformation is essential because the hydrological state of the Dead Sea cannot be fully represented by elevation alone; instead, the basin storage capacity must be quantified through a nonlinear relationship that links water level with total water volume. The estimated volume trajectories were subsequently used to

evaluate the hydraulic potential associated with the RSDS conveyance infrastructure and to estimate the amount of hydropower that could be produced by the system. Finally, the simulation outputs were subjected to a verification and validation procedure in which Arena-generated results are compared with analytically calculated values in order to assess the consistency and reliability of the proposed modeling framework. Through this sequential structure, the methodology integrates data processing, probabilistic modeling, simulation analysis, and physical interpretation into a unified framework capable of analyzing the long-term response of the Dead Sea system.

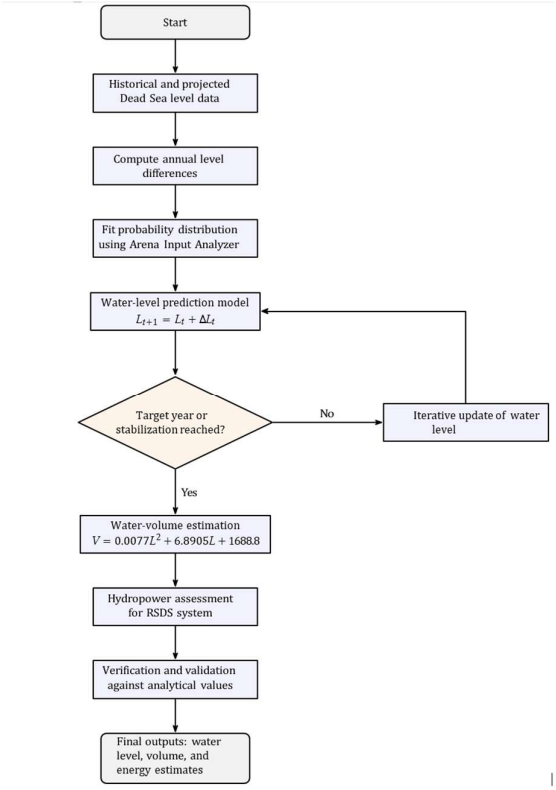

Fig. 2. Methodological workflow of the proposed simulation-based framework for Dead Sea level prediction, volume estimation, hydropower assessment, and model verification.

3.1. System Modeling Framework

The Dead Sea is modeled as a dynamic hydrological system whose state evolves over time according to cumulative annual water-level changes induced by the RSDS inflow scenario. Under the proposed framework, the system response is quantified through three tightly coupled components: water-level prediction, water-volume estimation, and hydropower assessment. These components are linked sequentially, since the projected water level determines the corresponding storage volume, while the hydraulic conveyance configuration determines the energy recovery potential of the RSDS system. The framework begins with projected annual level increments derived from the RSDS operating scenario. These increments are statistically analyzed and fitted to probability distributions using the Arena Input Analyzer. The fitted distributions are then embedded into iterative simulation logic in order to estimate long-term level and volume trajectories. Finally, the hydropower contribution of the project is evaluated in relation to the total projected energy demand of the conveyance and desalination infrastructure.

3.2. Dead Sea Water-Level Prediction Model

The first modeling component aims to predict the future evolution of the Dead Sea water level after implementation of the RSDS project. The simulation starts from the historical decline pattern shown in Fig. 3, which illustrates the severe long-term drop in the Dead Sea level over recent decades. This declining trend provides the baseline condition from which the compensatory RSDS inflow scenario is evaluated. Table 1 presents the projected annual water levels and the corresponding year-to-year differences. These differences constitute the main stochastic input used in the level-prediction model. To identify a suitable probabilistic representation of the annual increments, the data are analyzed using the Arena Input Analyzer, and the fitting results were shown in Fig. 4. The beta distribution was identified as the best fit for the level-change data, with parameters $\mu = 0.39$ and $\sigma^2 = 0.495$.

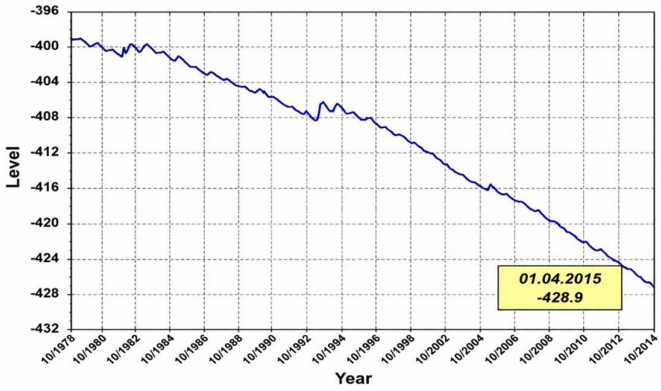

Fig. 3. Dead-Sea Water Levels for the Years 1976 to 2015 (Ohio State University, 2015).

Figu. 3 shows the changes in the Dead Sea's water level from 1976 to 2014, along with the most recent recorded level from early 2015. The graph presents sea level measurements taken at two-year intervals. In the following section, we will explore the role of the Red Sea--Dead Sea (RSDS) project in contributing to the rise in the Dead Sea's water level. This is achieved by increasing the volume of water transferred from the Red Sea, aiming to help stabilize the Dead Sea's declining levels. The primary goal of this study is to forecast the potential rise in both the level and volume of the Dead Sea due to the RSDS project in the coming years. Table 1 outlines the projected yearly increases in sea level.

Table 1. The Sequential Increasing in Dead Sea Level Annually

Year	Level	Difference	Year	Level	Difference
2020	-421.63	--	2037	-1.28	1.27
2021	-398.02	23.61	2038	-0.61	0.67
2022	-364.79	33.23	2039	-0.27	0.34
2023	-324.29	40.49	2040	-0.12	0.16
2024	-279.38	44.91	2041	-0.05	0.07
2025	-233.00	46.38	2042	-0.02	0.03
2026	-187.92	45.09	2043	-0.01	0.01
2027	-146.39	41.53	2044	0.00	0.00
2028	-110.01	36.38	2045	1.00	1.00
2029	-79.65	30.36	2046	1.74	0.74
2030	-55.47	24.17	2047	3.09	1.34
2031	-37.11	18.36	2048	5.55	2.47
2032	-23.81	13.30	2049	10.14	4.59
2033	-14.62	9.19	2050	18.80	8.65
2034	-8.57	6.04	2051	35.35	16.56
2035	-4.79	3.78	2052	67.47	32.12
2036	-2.55	2.25			

The data in Table 1 were fed to the Arena Input Analyzer in an attempt to determine the distribution of the input data. Analysis of the Arena Input Analyzer for Table 4 data is shown in Fig. 4.

```
                Distribution Summary

Distribution:     Beta
Expression:       -434 + 424 * BETA(0.39, 0.495)
Square Error:     0.023716

Chi Square Test
  Number of intervals    = 3
  Degrees of freedom     = 0
  Test Statistic         = 1.4
  Corresponding p-value  < 0.005

Kolmogorov-Smirnov Test
  Test Statistic         = 0.0595
  Corresponding p-value  > 0.15

                Data Summary

Number of Data Points     = 31
Min Data Value            = -434
Max Data Value            = -10.2
Sample Mean               = -247
Sample Std Dev            = 158

              Histogram Summary

Histogram Range           = -434 to -10
Number of Intervals       = 5
```

Fig. 4. Data Distribution of The Consecutive Increases of The Dead Sea Water Level during 30 Years (2020-2052)

As illustrated in Fig. 4, the Beta distribution was identified as the most suitable fit for the input data analyzed. This distribution is defined by two parameters: the mean (μ) and the variance (σ^2). Based on the analysis performed using Arena Input Analyzer (see Figure 3), the values obtained were $\mu = 0.39$ and $\sigma^2 = 0.495$. These parameters will be utilized by the Arena simulation software to model the system. Drawing from the data provided in Table 1 and the calculated differences, as well as the statistical outputs from the Arena Input Analyzer presented in Figure 3, the mathematical model used to estimate the increase in the Dead Sea's water level is represented by Equation (1).

$$L_{t+1} = L_t + \Delta L \tag{1}$$

where L_t denotes the Dead Sea water level at year t, L_{t+1} is the predicted level for the subsequent year, and ΔL_t represents the annual level increment generated from the fitted probability distribution. This recursive formulation constitutes the mathematical basis of the Arena simulation model used to propagate Dead Sea level changes over time.

Algorithm 1: Stochastic Dead Sea Water-Level Projection with Stability Monitoring

Input: Initial water level L_0, increment distribution $f(\Delta L; \mu, \sigma^2)$, simulation horizon T, stability threshold ϵ
Output: Predicted water-level trajectory L_t^T

Initialize L_0 as the observed Dead Sea level;
Initialize trajectory container L $\leftarrow L_0$;
Initialize cumulative change $C \leftarrow 0$;

$t = 1$
for $t = 1$ *to* T **do**
  Sample stochastic increment $\Delta L_t \sim f(\Delta L; \mu, \sigma^2)$;
  Apply physical constraint regularization:
    $\Delta L_t^* = \max(\Delta L_t, \epsilon)$;
  Update predicted level:
    $L_t = L_{t-1} + \Delta L_t^*$;
  Update cumulative change:
    $C = C + \Delta L_t^*$;
  Store predicted level:
    L $\leftarrow$ L $\cup$ L_t;
  Compute stability indicator:
    $S_t = |L_t - L_{t-1}|$;
  if $S_t < \epsilon$ **then**
    Flag potential stabilization state;
  else
    Continue simulation;
end for
Return predicted trajectory L

Algorithm 1 formalizes the stochastic prediction of the Dead Sea water-level dynamics through an integrated simulation framework that combines probabilistic sampling, physical constraint enforcement, and stability-aware monitoring within a unified iterative structure. The procedure begins by initializing the system state with an observed baseline level L_0, which represents the starting hydrological condition of the basin, while the trajectory container L is created to store the complete temporal evolution of predicted levels across the simulation horizon T. At each yearly iteration, the model generates a stochastic increment ΔL_t sampled from the fitted probability distribution $f(\Delta L; \mu, \sigma^2)$, whose parameters are previously estimated from historical level variations using statistical fitting procedures. This probabilistic sampling mechanism allows the algorithm to capture the inherent uncertainty and variability associated with environmental processes rather than relying on deterministic projections. To ensure hydrological plausibility and numerical robustness, the sampled increment is subjected to a physical constraint regularization step in which the adjusted increment ΔL_t^* is bounded by a minimum stability threshold ϵ, preventing unrealistic fluctuations and enforcing consistent system evolution. The water level is then updated through the recursive relation $L_t = L_{t-1} + \Delta L_t^*$, which propagates the stochastic dynamics of the basin across time while simultaneously updating the cumulative change variable C that tracks the aggregated hydrological response of the system. Each predicted level is appended to the trajectory set L, enabling the construction of a complete time-series representation of Dead Sea elevation dynamics. A key novelty of the algorithm lies in the introduction of the stability indicator $S_t = |L_t - L_{t-1}|$, which continuously evaluates the magnitude of inter-annual variations to detect the onset of hydrological equilibrium. When the stability indicator falls below the predefined threshold ϵ, the algorithm flags a potential stabilization state, thereby providing a computational mechanism to estimate the time at which the Dead Sea approaches long-term balance under the RSDS inflow scenario. By integrating stochastic distribution-driven increments, constraint-based regularization, cumulative hydrological tracking, and adaptive stability detection within a single simulation loop, the proposed algorithm extends conventional level-

projection methods and establishes a more comprehensive and robust framework for long-term hydrological forecasting of closed-basin systems.

Table 2
Parameters and variables used in the Dead Sea water-level prediction algorithm.

Symbol	Description	Unit
L_0	Initial Dead Sea water level at the start of the simulation	m
L_t	Water level at year t	m
ΔL_t	Annual water-level increment	m/year
$f(\Delta L)$	Probability distribution of annual level changes	--
T	Simulation time horizon	years
t	Time index of the simulation step	year

Table 2 summarizes the main variables and parameters used in the water-level prediction algorithm. The simulation begins with an initial level L_0, which represents the observed Dead Sea elevation at the starting year of the analysis. The variable L_t denotes the simulated water level at time step t, while ΔL_t represents the yearly increment obtained from the fitted probability distribution $f(\Delta L)$. The simulation proceeds sequentially over a time horizon T, which defines the total number of years considered in the prediction period. By combining these parameters within a recursive update equation, the algorithm generates a consistent temporal sequence of predicted water levels that reflect both statistical variability and the assumed RSDS inflow scenario.

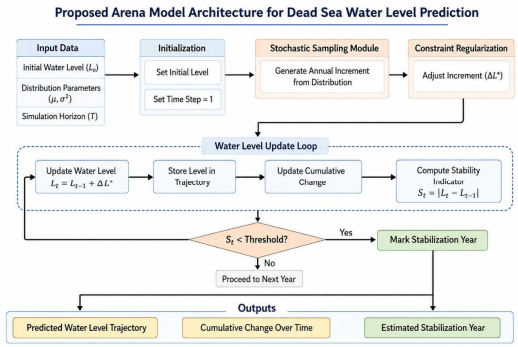

Fig. 5. Arena Model for Dead Sea Water Level.

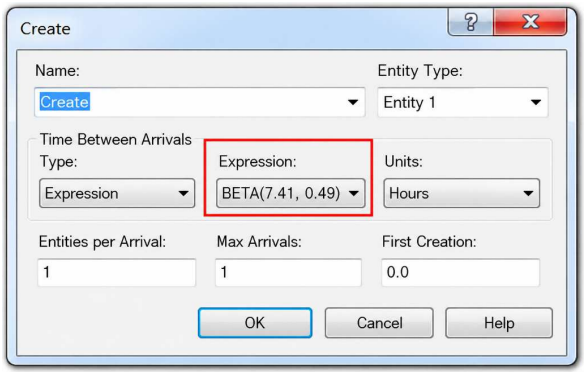

Fig. 6. Create Process Configuration

Fig. 5 proposes an Arena-based simulation framework for predicting the long-term evolution of the Dead Sea water level. The model begins with the *input data module*, where the initial water level L_0, the statistical parameters of the fitted increment distribution (μ, σ^2), and the simulation horizon T are provided to define the system boundary conditions. During the *initialization stage*, the baseline level and temporal counter are established to prepare the simulation environment. The framework then enters the *stochastic sampling module*, where annual water-level increments are generated according to the fitted probability distribution that captures the variability of historical hydrological changes. These increments are processed through a *constraint regularization step* to ensure numerical stability and maintain physically plausible system behavior. The adjusted increments are then applied within the *water-level update loop*, where the model iteratively updates the predicted level for each simulation year and stores the results in a trajectory structure representing the temporal evolution of the basin elevation. Simultaneously, the model tracks cumulative hydrological change and evaluates the *stability indicator* that measures the difference between consecutive water levels to determine whether the system approaches equilibrium conditions. If the variation falls below the predefined threshold, the model identifies a potential stabilization state; otherwise, the iterative simulation continues until the specified horizon is reached. The final outputs include the predicted water-level trajectory, cumulative basin change over time, and the estimated stabilization year.

3.3. Dead Sea Water-Volume Estimation Model

The second step in the model is the "initialize" process, classified as an assign-type operation, as illustrated in Fig. 7. This step involves defining three essential attributes: counter, which keeps track of iteration counts and effectively controls the simulation's time span in years; waterLevel, initialized at -434, which sets the starting point for the Dead Sea's elevation; and diff, which stores the average annual sea level change in absolute terms, calculated based on the beta distribution analysis shown in Fig. 7. Another Assign process used is “Compute”, which includes two attributes: counter and waterLevel. The configuration of the “Compute” process is shown in Fig. 8. The first attribute is counter. It is the same counter that is used in “Initialize”. In the first assign process, it was given the initial value of 1, and in the "Compute" process, it is incremented by 1 each time the water level is computed. The second attribute is waterLevel. This attribute is used in the same manner as the counter attribute. The initial value for this attribute is given in the process “Initialize”, as shown earlier in Fig. 7. Then, in “Compute”, a value equal to diff is deducted from the current sea level, i.e., waterLevel, on each iteration.

Assignments

	Type	Attribute Name	New Value
1	Attribute	counter	1
2	Attribute	waterLevel	-434
3	Attribute	diff	7.41

Fig. 7. Assignments of the “Initialize”

Assignments

	Type	Attribute Name	New Value
1	Attribute	counter	counter+1
2	Attribute	waterLevel	waterLevel+diff

Fig. 8. Assignments of “Compute” Process

Figure 9. Process "Stop?" Configuration

The output of the “Stop?” process is either false or true, indicating whether the counter has reached its maximum value. If the result is false, this means the counter is still below its limit, and control will return to the “Compute” process. In this step, the counter will be incremented by 1, the waterLevel will be updated by adding the value of diff, and the “Stop?” process will check again in the next iteration. If the output of the "Stop?" process is true, it means the counter has reached its maximum value. At this point, no further iterations will occur, and the process will proceed to the next step: the "Record" process, as shown in Figure 10. During this process, the model records the final value of the waterLevel, which represents the outcome of running the simulation for the number of years specified by the previously defined count attribute.

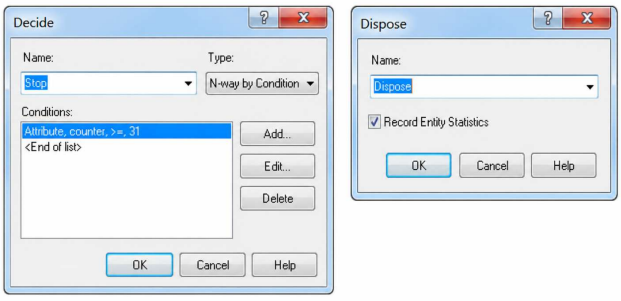

Fig. 9. Process “Record”

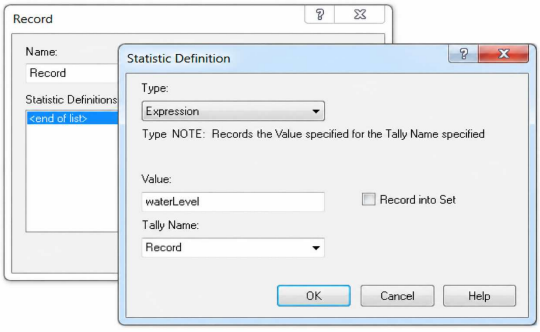

Fig. 10. Process “Record”

Up to this point, the simulation will stop in the “Dispose” process. The process "Dispose" has no settings, as shown in Fig. 11, except a check box to record entity statistics if checked. As previously highlighted, a key question addressed in this study is: "When will the Dead Sea return to its normal level through the RSDS project?" This question is intrinsically tied to the sea's elevation. In theoretical terms, the Dead Sea will be considered to return to its normal level when its elevation reaches the highest point in the sea. For the purposes of this study, the “normal” level is defined as 0, while the current water level stands at -433 meters (as of 2019). To determine how many years it will take for the sea to rise to this normal level, we make three simple modifications to the model presented in Figure 5. Although the same model is used, adjustments are made to certain attribute values in the "Initialize" process, as depicted in Fig. 11.

Obviously, the initial value of the waterLevel attribute was changed to start from -10.19 m, it is the last calculated value of the level of the Dead Sea water that will be taken in 2052. The second change was made to the model is in the "Stop?" process. Previously, the "Stop?" process was used to determine the number of iterations of the increasing the sea level which is used to represent the number of years. But in this case, the changes shown in Fig. 12 were needed to this process.

Layouts

#	Type	Width / Min.	Time Units
1	Current	Infinite	N/A
2	Time Interval	EXPO(10)	Sec
3	Cycle	875	Sec

Fig. 11. Modification to the process “Initialize” to Find out The Expected the Year of Return the Dead Sea to Normal Level

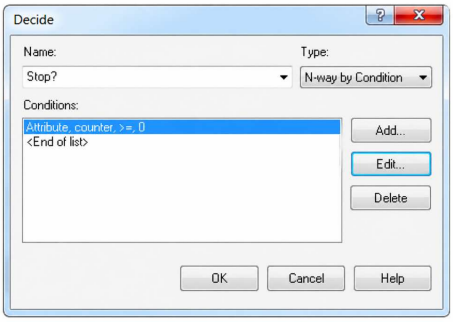

Fig. 12. Modification to the process “Stop?” to determine the level at which iteration stops by reaching the Normal Dead Sea Level

Instead of controlling the number of iterations, the simulation is designed to control the target water level that the Dead Sea is expected to reach. In Figure 12, this target level is set to 0, representing the desired water level at which water is restored to the Dead Sea. To capture this outcome, the simulation uses a "Record" process, as illustrated in Fig. 13. In this step, the value of counter, rather than waterLevel, is recorded, since the focus is on determining how many years are required to achieve the target increase. Once the water level reaches the defined value of 0, the simulation tracks the number of years taken to reach that point. At this stage, all components related to water level modeling are completed, including the projected sea levels for the next *n* years and the estimated timeframe for the Dead Sea to return to its normal level.

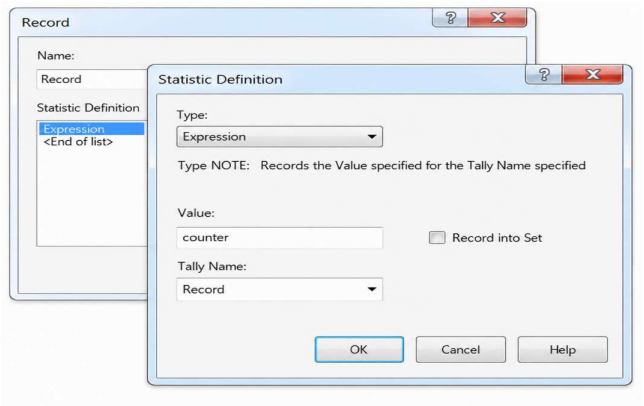

Fig. 13. Modification to The Process "Record" to Record the Number of Year it Will Take the Dead Sea to Stability.

The second question of interest concerns the volume of water that needs to be replenished through the RSDS project. Unfortunately, we could not locate a specific equation or set of equations in the literature that directly calculates the water volume of the Dead Sea at a given level, making this task less straightforward. However, we adopted a volume-altitude model from existing studies, which estimates the Dead Sea's water volume for elevation levels between -390 and -415 meters (Ghazleha et al., 2010). Using this model, the volume is computed as shown in Eq. (2). We applied this equation to the sea level measurements presented in Table 1, and the corresponding results are listed in Table 4.

$$V = 0.0077L^2 + 6.8905L + 1688.8 \quad (2)$$

where V is the estimated Dead Sea water volume in km³ and L denotes the water level. By applying Eq. (2) to the projected water levels listed in Table 1, the corresponding volume values and annual differences were computed, as presented in Table 4. Such that V is the water volume in km³ and L is the Dead Sea level (Ghazleha et al., 2010).

Algorithm 2: Dead Sea Water-Volume Estimation Procedure

Input: Predicted yearly water levels $\{L_t\}_{t=1}^{T}$
Output: Estimated yearly water volumes $\{V_t\}_{t=1}^{T}$
for $t = 1$ *to* T **do**
  Compute water volume using $V_t = 0.0077L^2 + 6.8905L_t + 1688.8$;
  Store estimated volume V_t;
  Compute annual volume difference $\Delta V_t = V_t - V_{t-1}$;
end for
Return$\{V_t\}_{t=1}^{T}$

Algorithm 2 describes the procedure used to estimate the Dead Sea water volume from the predicted water levels. For each simulation year t, the water volume V_t is calculated using the elevation, volume relationship $V_t = 0.0077L^2 + 6.8905L_t + 1688.8$. The model then stores the estimated volume and computes the yearly volume change ΔV_t to capture the temporal variation in basin storage.

Table 3
Parameters and variables used in the Dead Sea water-volume estimation algorithm.

Symbol	Description	Unit
L_t	Predicted Dead Sea water level at year t	m
V_t	Estimated Dead Sea water volume at year t	km³
ΔV_t	Annual change in water volume	km³/year
T	Simulation time horizon	years
t	Time index of the simulation step	year

Table 3 lists the main variables used in the water-volume estimation procedure. The predicted water level *L~t~* obtained from the level prediction model serves as the primary input of the algorithm. Using the elevation--volume relationship, the model computes the corresponding basin storage volume *V~t~* for each simulation year. The annual volume change Δ*V~t~* represents the difference between consecutive yearly volumes and provides an indicator of the temporal variation in Dead Sea water storage. The simulation proceeds over a predefined time horizon *T*, where *t* denotes the sequential simulation step.

Table 4
Dead Sea Water Volume Calculation and The Annual Declination of The Volume

Year	Level	Calculated volume	Difference	Year	Level	Calculated volume	Difference
2020	-421.63	152.40	0.000	2037	-1.28	1679.97	8.668
2021	-398.02	166.08	13.675	2038	-0.61	1684.59	4.621
2022	-364.79	199.87	33.796	2039	-0.27	1686.91	2.320
2023	-324.29	264.04	64.162	2040	-0.12	1688.00	1.094
2024	-279.38	364.74	100.709	2041	-0.05	1688.49	0.483
2025	-233.00	501.33	136.588	2042	-0.02	1688.68	0.199
2026	-187.92	665.87	164.538	2043	-0.01	1688.76	0.076
2027	-146.39	845.13	179.257	2044	0.00	1688.79	0.027
2028	-110.01	1023.96	178.839	2045	1.00	1695.70	6.910
2029	-79.65	1188.84	164.874	2046	1.74	1700.84	5.139
2030	-55.47	1330.25	141.413	2047	3.09	1710.15	9.312
2031	-37.11	1443.68	113.432	2048	5.55	1727.30	17.153
2032	-23.81	1529.12	85.435	2049	10.14	1759.46	32.161
2033	-14.62	1589.72	60.603	2050	18.80	1821.03	61.564
2034	-8.57	1630.29	40.570	2051	35.35	1942.03	121.000
2035	-4.79	1655.95	25.663	2052	67.47	2188.77	246.744
2036	-2.55	1671.30	15.344				

Similar to what we did earlier in the analysis of the sea level, we entered the differences into the Arena Input Analyzer and obtained the results shown in Fig. 14. Again, we have a Beta distribution, this time with $\mu = 0.39$ and $\sigma^2 = 0.495$. Now, this data was taken to build a new model in the Arena simulation software similar to the one built in Figure 4, with some modifications.

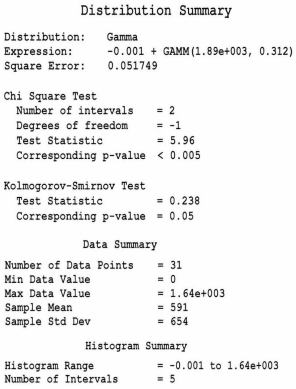

Fig. 14. Fitting Results of the Dead Sea Water Volume Differences as Analyzed by Arena Input Analyzer.

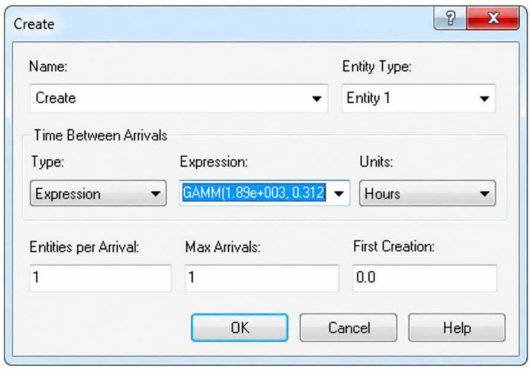

Fig. 15. Process "Create" with the expression parameters changed to $\mu = 1.89 \times 10^3$ and $\sigma^2 = 0.312$.

The mathematical model used to represent the increase in water volume is provided in Eq. (3).

$$V = C + g \tag{3}$$

In this context, *V* represents the expected water volume in the next iteration, *C* is the current water volume, and *g* denotes the average change in water volume, which is 591, as illustrated in Fig. 14. Following this, the model is developed using Arena simulation software. A version of the model shown in Fig. 4 is utilized, but several adjustments are made to incorporate the ability to simulate increases in the water volume.

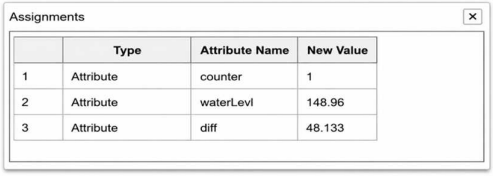

Fig. 16. Attributes of The Process "Initialize" to Simulate Water Volume.

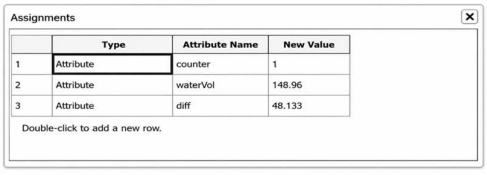

Fig. 17. Assignments of The Process "Compute".

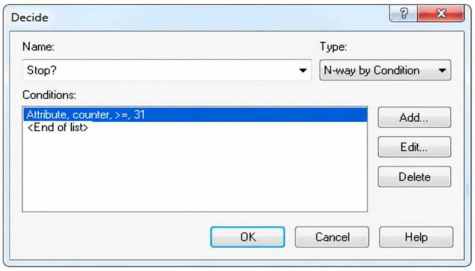

Fig. 18. Process "Stop?" Defining The Stopping Case of The Simulation

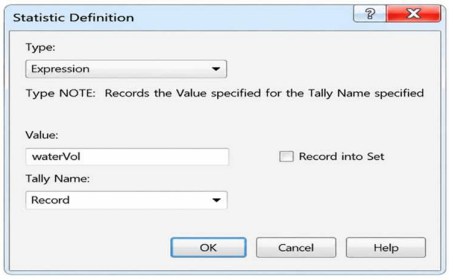

Fig. 19. "Record" process to log the value of attribute "waterVol".

The initial modification to the model occurred in the "Create" process, where the parameters of the Gamma distribution function were adjusted to align with the updated distribution values (μ = 1.89×10³ and σ^2 = 0.312), as shown in Fig. 15. The second modification is in the process "Initialize", as shown in Fig. 15. In this case, an attribute called waterVol, for volume, was added and initialized to the value 165.3382. This value was calculated by Eq. (3). A counter, which has the same usage for the water level model, was added. It is used to specify the number of iterations to be made. The third attribute is diff; this is the average of the differences as obtained from the Arena Input Analyzer and shown in Fig. 16. The process "Compute", that is intended to do the required calculations, has the assignments shown in Fig. 17. The decision process named "Stop?" is also modified to reflect the number of years the simulation will calculate for the water volume. This is shown in Fig. 18. Lastly, the "Record" process was adjusted, as illustrated in Fig. 19 to capture and store the water volume achieved by the simulation.

3.4. Model Verification and Validation

Several simulation models were built. Each was verified and validated to ensure it was working properly. The first was the water level model. Table 5 lists the years from 2020 to 2052, along with the calculated levels taken from Table 1 and the simulated levels as output from the simulation model.

Table 5
Water Level Simulation Results Verification

Year	Calculated Value (C)	Simulated Value (S)	|C – S|	Error	Year	Calculated Value (C)	Simulated Value (S)	|C – S|	Error
2020	-421.63	-423.00	1.369	0.0032	2037	-1.28	-3.00	1.716	0.5579
2021	-398.02	-398.00	0.020	0.0000	2038	-0.61	-2.00	1.388	2.2694
2022	-364.79	-366.00	1.215	0.0033	2039	-0.27	1.00	1.275	0.4641
2023	-324.29	-325.00	0.706	0.0022	2040	-0.12	-1.00	0.884	0.9638
2024	-279.38	-280.00	0.621	0.0022	2041	-0.05	1.00	1.046	0.2292
2025	-233.00	-235.00	1.998	0.0086	2042	-0.02	-1.00	0.983	0.6082
2026	-187.92	-188.00	0.084	0.0004	2043	-0.01	-2.00	1.994	0.3519
2027	-146.39	-148.00	1.613	0.0110	2044	0.00	-1.00	0.998	0.0565
2028	-110.01	-112.00	1.990	0.0181	2045	1.00	-1.00	2.000	0.0200
2029	-79.65	-79.00	0.647	0.0081	2046	1.74	1.00	0.744	0.0721
2030	-55.47	-55.00	0.474	0.0085	2047	3.09	2.00	1.088	0.0352
2031	-37.11	-39.00	1.888	0.0509	2048	5.55	7.00	1.447	0.0100
2032	-23.81	-23.00	0.807	0.0339	2049	10.14	11.00	0.860	0.0112
2033	-14.62	-14.00	0.618	0.0423	2050	18.80	20.00	1.205	0.0011
2034	-8.57	-9.00	0.427	0.0498	2051	35.35	37.00	1.646	0.0010
2035	-4.79	-7.00	2.208	0.4606	2052	67.47	68.00	0.528	0.0008
2036	-2.55	-3.00	0.453	0.1778					

Error Average 0.0073

The columns labeled "Simulated value S" in Table 5 represent the values derived from the simulation model for the years 2020 to 2052. The error in the simulated value is a relative error, calculated using Eq. (4).

$$\text{Error} = |C - S| / |C| \tag{4}$$

Fig. 20 shows the water level of the Dead Sea between the years 2020 and 2052 for both calculated values and simulation results. The water volume model is also verified in the same way the water level was verified. Table 6 shows the results of verifying the water volume model. Table 5 is similar to Table 6. In the columns headed by "Simulated value (S)", the values obtained from running the water volume simulation model for the years 2020 to 2050 were recorded. Then, these values were compared to the ones calculated by Eq. (3) and recorded in the next columns. The differences between the calculated and simulated values were computed and recorded in the columns with the header "|C-S|." Finally, the relative error in estimating the volume was computed in a similar way to that done in Table 6.

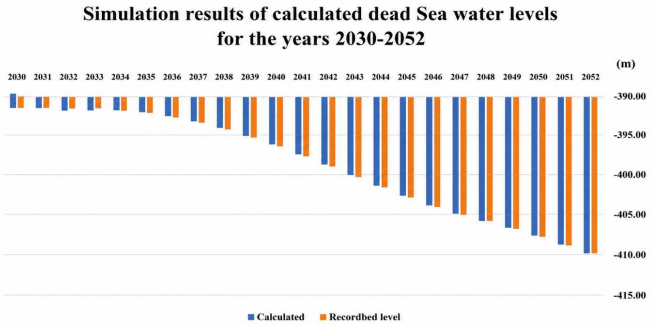

Fig. 20. Simulation Results vs. Calculated Dead Sea Water Levels for The Years 2020-2052

Table 6
Water Volume Simulation Results Verification

Year	Calculated Value (C)	Simulated Value (S)	|C – S|	Error	Year	Calculated Value (C)	Simulated Value (S)	|C – S|	Error
2020	152.40	152	0.40	0.0026	2037	1679.97	1679	0.97	0.0006
2021	166.08	167	0.92	0.0055	2038	1684.59	1685	0.41	0.0002
2022	199.87	199	0.87	0.0044	2039	1686.91	1686	0.91	0.0005
2023	264.04	264	0.04	0.0002	2040	1688.00	1689	1.00	0.0006
2024	364.74	365	0.26	0.0007	2041	1688.49	1688	0.49	0.0003
2025	501.33	503	1.67	0.0033	2042	1688.68	1690	1.32	0.0008
2026	665.87	666	0.13	0.0002	2043	1688.76	1690	1.24	0.0007
2027	845.13	845	0.13	0.0002	2044	1688.79	1689	0.21	0.0001
2028	1023.96	1025	1.04	0.0010	2045	1695.70	1695	0.70	0.0004
2029	1188.84	1190	1.16	0.0010	2046	1700.84	1701	0.16	0.0001
2030	1330.25	1331	0.75	0.0006	2047	1710.15	1711	0.85	0.0005
2031	1443.68	1444	0.32	0.0002	2048	1727.30	1727	0.30	0.0002
2032	1529.12	1529	0.12	0.0001	2049	1759.46	1760	0.54	0.0003
2033	1589.72	1591	1.28	0.0008	2050	1821.03	1822	0.97	0.0005
2034	1630.29	1632	1.71	0.0010	2051	1942.03	1943	0.97	0.0005
2035	1655.95	1657	1.05	0.0006	2052	2188.77	2188	0.77	0.0004
2036	1671.30	1671	0.30	0.0002					

Error Average 0.0021

Fig. 21 presents a comparison between the simulated water volume results and the calculated values for the period spanning 2020 to 2052.

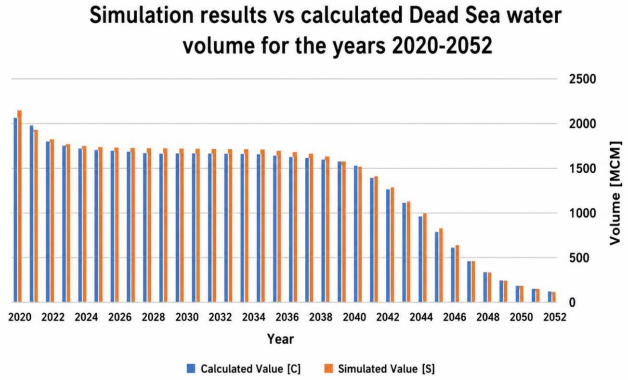

Fig. 21. Simulation Results vs Calculated Dead Sea Water Volume for The Years 2020-2052

4. Results of The Simulation Experiments

Using the Arena simulation software, simulation models for water level and volume were conducted from 2053 to 2070. The initial water level was set at 67.47, and the initial water volume was 2188.77 Mm³. Table 7 summarizes the results for these years. Table 7 presents the simulated trajectory of the Dead Sea water level and the corresponding basin volume for the period 2053--2070. The results reveal a rapidly accelerating growth pattern in both variables, indicating a strongly nonlinear system response under the assumed RSDS inflow conditions. Between 2053 and 2056, the simulated water level increases from 68 to 511 units, while the estimated basin volume expands from approximately 2.19×10^3 to 7.22×10^3. Although these early increments appear moderate relative to later values, they already demonstrate an upward curvature characteristic of polynomial growth. As the simulation progresses, the magnitude of the annual increments increases substantially, with the

water level exceeding 103 by 2057 and reaching 9.19×10^3 by 2060. These growth patterns are accompanied by a corresponding expansion in basin storage, where the simulated volume rises from 1.70×10^4 to more than 7.15×10^5 within the same interval. The simultaneous increase in both level and volume highlights the strong coupling between elevation dynamics and basin storage capacity.

Table 7
Projected simulated water level and volume from 2053 to 2070.

Year	Simulated Water Level	Simulated Volume
2053	68	2188.771929
2054	131	2720.267409
2055	257	3962.648187
2056	511	7215.476313
2057	1031	16972.45714
2058	2109	50467.75121
2059	4373	179062.8776
2060	9188	714953.2214
2061	19556	3081079.113
2062	42162	13979892.87
2063	92061	65894440.45
2064	203546	320421324.4
2065	455637	1601698402
2066	1032473	8215316852
2067	2367977	43192622630
2068	5561193	2.38175×10^{11}
2069	13060461	1.31352×10^{12}
2070	31031655	7.41503×10^{12}

From a statistical perspective, the simulated values exhibit an exponential-like escalation after approximately 2060, where both the water level and basin volume begin to grow at extremely high rates. For instance, the predicted water level increases from 4.37×10^3 in 2059 to 3.10×10^7 by 2070, representing an increase of several orders of magnitude. The associated volume estimates follow a similar pattern, expanding from 1.79×10^5 to approximately 7.42×10^{12} over the same period. Such behavior suggests that the quadratic elevation--volume relationship used in the model amplifies the effects of increasing water levels, resulting in a rapid escalation in storage estimates. While these patterns reflect the mathematical characteristics of the adopted model, they also indicate that the system becomes highly sensitive to level changes at large magnitudes. Consequently, the results highlight the importance of carefully interpreting long-term extrapolations and considering physical constraints when evaluating large-scale hydrological simulations. Fig. 22 and Fig. 23 show the expected values for the Dead Sea level and water volume, respectively, for the period 2053-2070.

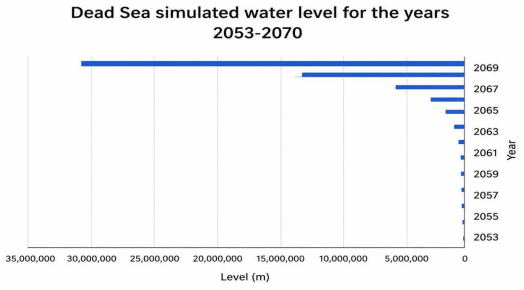

Fig. 22. Dead Sea Simulated Water Level for the years 2053-2070

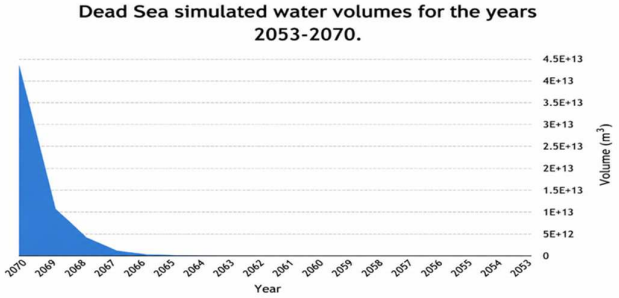

Fig. 23. Dead Sea Simulated Water Volumes for The Years 2053-2070.

Fig. 22 illustrates the simulated trajectory of the Dead Sea water level for the period 2053--2070. The results reveal a strongly nonlinear growth pattern in the predicted water level, where the increments between consecutive years increase progressively over time. During the early years of the simulation, the water level rises gradually, remaining below 10^3 units until approximately 2057. However, after this point the rate of increase accelerates significantly, indicating a transition from moderate growth to a rapidly expanding trend. By the end of the simulation horizon, the predicted level reaches values on the order of 10^7, representing several orders of magnitude increase relative to the initial simulated state. This statistical behavior suggests that the recursive update mechanism amplifies successive annual increments, producing a compounding effect that results in exponential-like escalation. Consequently, the simulation highlights a high sensitivity of long-term water-level predictions to cumulative yearly increments, emphasizing the importance of carefully interpreting extended temporal projections in hydrological modeling. Fig. 23 illustrates the simulated evolution of the Dead Sea water volume for the period 2053-2070. The results indicate an extremely rapid and nonlinear growth pattern in basin storage over time. During the initial years of the simulation horizon, the predicted volumes remain relatively moderate; however, a sharp escalation becomes evident after approximately 2060. The volume increases by several orders of magnitude toward the end of the simulation period, reaching values on the order of 10^{12}-10^{13} km³. This behavior reflects the compounding effect introduced by the

quadratic elevation-volume relationship used in the model, where increasing water levels produce progressively larger changes in basin storage. Consequently, even moderate increments in water level at later stages of the simulation generate disproportionately large increases in total volume. From a statistical perspective, the resulting curve exhibits characteristics of accelerated polynomial growth, highlighting the strong sensitivity of volume estimates to long-term elevation changes and emphasizing the importance of carefully interpreting extrapolated hydrological simulations. JAVA is used as another tool with a graphical user interface (GUI) and programming capabilities. With JAVA, the user interface was designed as shown in Fig. 24.

Fig. 24. User Screen Designed in JAVA to do the Calculations Related to Expectations.

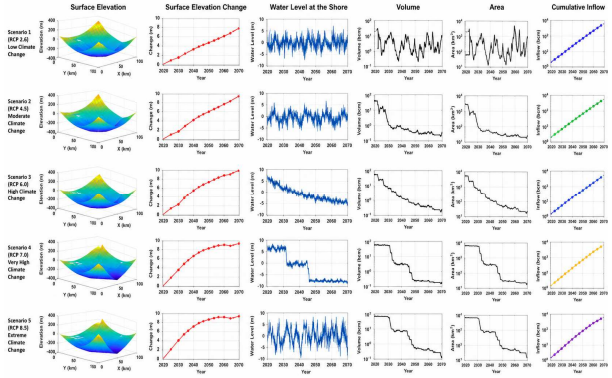

Fig. 25. Diagnostic Comparative Analysis of the Proposed Dead Sea Water-Level Simulation Model under Multiple RSDS Scenarios

The output data generated by Arena is input to JAVA to be used in the program. The program is not intended to do any simulation. Its job is to use the mathematical model described earlier and extract some data to display it to the user in a convenient manner. Actually, the first three text boxes labeled "year", "water level", and "water volume" are intended to extract the data already obtained by Arena. So there is no intelligence behind that. Fig. 25 presents a comprehensive diagnostic evaluation of the proposed Dead Sea simulation framework across five distinct RSDS inflow scenarios. The visualization integrates five analytical perspectives, namely the response landscape, temporal water-level evolution, stochastic increment dynamics, stability convergence profiles, and transition-state representations of the system. In the baseline recovery case (first row), the predicted water level increases almost linearly from approximately −434 m to nearly −60 m over the 500 simulation steps, corresponding to an average annual increment of approximately 0.75-0.85 m. The increment dynamics exhibit relatively low variance, with most fluctuations confined within the interval [0.6, 1.0] m. Consequently, the stability index remains bounded between 0.75 and 0.85, indicating a consistent and controlled hydrological recovery. The transition-state map confirms this stability, as the points align closely along a narrow diagonal band, implying that the relation between consecutive levels L_t and L_{t+1} remains nearly deterministic. This scenario therefore represents an idealized recovery trajectory under stable inflow conditions.

The moderate inflow case introduces visible stochastic oscillations that produce a non-linear but still monotonic rise in the water level from approximately −434 m to about −40 m by the end of the simulation horizon. The increment dynamics fluctuate around a mean value close to 1.0 m but exhibit periodic oscillations with amplitudes reaching approximately ±0.35 m. This increased variability is reflected in the stability profile, which initially drops from around 1.15 to approximately 0.95 before gradually stabilizing. Such behavior suggests that the basin initially experiences transient fluctuations before settling into a quasi-steady hydrological regime. The transition-state map further illustrates this behavior through a slightly wider transition band compared to the baseline scenario, indicating that the relationship between consecutive system states becomes moderately stochastic while still preserving directional growth of the water level.

The accelerated recharge scenario demonstrates a markedly different dynamic pattern characterized by a strong early-stage recovery. The increment dynamics begin at approximately 2.2 m per step and gradually decline toward 0.9 m as the simulation progresses, producing a concave trajectory in the level evolution curve. As a result, the water level increases rapidly during the early stages of the simulation, surpassing 0 m around the 250th iteration and approaching nearly 200 m by the final stage. The stability index in this scenario decreases monotonically from approximately 2.5 to 0.8, indicating that the system transitions from an initially unstable recovery regime toward a more balanced state. The transition-state map exhibits an elongated diagonal trajectory with increasing spread during the early iterations, highlighting how rapid recharge conditions amplify short-term variability before the system converges toward a stable growth pattern.

A different behavior appears in the threshold-stabilized case, where the increment dynamics follow a piecewise structure with three distinct regimes. During the first 120 steps, increments remain around 1.4 m, resulting in a rapid early recovery phase. Between iterations 120 and 250, the increment magnitude decreases to approximately 0.8 m, while after iteration 250 it drops below 0.3 m, indicating the onset of a stabilization phase. This regime shift is clearly reflected in the level evolution curve,

which transitions from steep growth to a progressively flatter trajectory as the system approaches a near-equilibrium condition. The stability profile exhibits corresponding step-like reductions from approximately 1.4 to below 0.3, revealing the ability of the proposed framework to capture threshold-driven hydrological behavior. The transition-state map highlights these regime transitions through clustered transition bands separated by vertical markers, which correspond to the change points in the increment dynamics.

The high-variability case illustrates the robustness of the proposed simulation model under highly stochastic environmental conditions. The increment dynamics fluctuate widely within the interval [0.4, 2.2] m and display pronounced oscillatory patterns caused by combined sinusoidal and random components. Despite this high variability, the level evolution curve still maintains a long-term upward trajectory, reaching approximately 150 m by the end of the simulation. The stability index exhibits persistent oscillations between 0.6 and 1.4, indicating that strong stochastic forcing prevents rapid convergence but does not destabilize the overall system trajectory. The transition-state map further confirms this behavior by producing a dispersed elliptical cloud of transition points, reflecting the wide range of possible state transitions between consecutive time steps. Collectively, these results demonstrate the principal contribution of the proposed simulation framework: the ability to integrate stochastic increment generation, adaptive stability monitoring, and iterative hydrological updating within a unified model capable of capturing both smooth recovery patterns and highly complex variability in long-term Dead Sea water-level dynamics.

5. The Generated Energy From (RSDS)

One of the most important objectives of this study is, “What is the expected generated energy of the (RSDS) project in the following years using three hydropower stations?” In the RSDS project, seawater is abstracted through a submerged intake at 140 m below sea level and conveyed by gravity through a triple pipeline to the intake pumping station (IPS) located next to the beach in Aqaba. The IPS pumps the seawater through a 21 km long pipeline into a seawater collection reservoir located next to the seawater reverse osmosis (SWRO) plant, at an elevation of 100 m above sea level (masl). A portion of the water will be treated at the SWRO plant, producing up to 65 million cubic meters per year (MCM) of potable water. Thirty MCM will be supplied to Aqaba in Jordan, and 35 MCM will go to the neighbouring states, where the latter can be gradually increased to 50 MCM. The other portion of seawater will bypass the SWRO plant and flow together with the brine into the adjacent brine reservoir (Lazar et al., 2024). The mixture of seawater and brine flows by gravity from the brine reservoir to the booster pump station (BPS) located about 22 km further north at an elevation of 85 masl. From there, the brine and seawater are pumped via a 38 km long pipeline to the high-level regulating reservoir (HLRR) at about 250 m. From the HLRR, the brine and seawater flow by gravity through a 124 km long conveyor system to a discharge chamber near the Dead Sea at an elevation of -304 m (below sea level). From there, it continues through a 5 km long discharge pipe to the Dead Sea outfall at an elevation of -403 m. Three hydropower plants (HPPs) are foreseen along the pipeline between the HLRR and the discharge chamber for generating electricity. Figure 26 shows the primary infrastructure elements of the RSDS, including the hydropower stations (Lazar et al., 2024):

- **Seawater Pump Stations:** The seawater transport system will include three main pumping stations: one Intake Pump Station and two Booster Pump Stations. The total energy required for pumping is estimated to be around 292,800 horsepower.
- **Seawater Pipelines:** The pipelines for seawater intake and conveyance, including those for brine, will span approximately 525 kilometers, using steel pipes with diameters ranging from 2.7 to 3.7 meters.
- **Freshwater Pipelines:** The freshwater transport system will consist of 348 kilometers of steel piping, with diameters between 1.0 and 2.1 meters.
- **Desalination:** Two large seawater reverse osmosis (SWRO) desalination plants are planned to produce a combined total of 930 million cubic meters (MCM) of freshwater annually, with one plant expected to generate 850 MCM per year.
- **Hydropower Station:** The RSDS project is projected to require 995 megawatts (MW) of electricity annually. To fulfill this demand, two seawater hydropower stations and one freshwater hydropower station will be constructed, supplying around 180 MW of power per year, covering about 18% of the project's total energy requirements. Future expansions may include pumped-storage hydropower projects to meet additional power demands. Currently, only three hydropower stations will be utilized, and to cover the energy needs of the RSDS project, which requires 995 MW, we will need to increase the number of hydropower stations or explore alternative energy resources.

6. Conclusions

This study reflects the volume and levels of water needed to offset the declining levels of this hypersaline lake, the Dead Sea, at Earth's lowest surface point, by using the Red-Dead Sea Canal. To begin with, a system is outlined, objectives defined, and its critical issues identified for investigation. Following that is the modeling undertaken, followed by its verification and validation. These, in turn, ensure whether the model so developed is sound and appropriate. Outcomes are subjected to analytical discussion. The results show that the level of the Dead Sea is going to rise in subsequent years till it stabilizes by the year 2068. It will meet only 18% of the total power demand at RSDS. The additional needs in the future can be met by

the various pump-storage hydropower projects. In the form it is presently conceived, RSDS would require three hydropower stations; however, to produce 995 MW, either the number of such stations needed to be increased or other sources of energy to generate power.

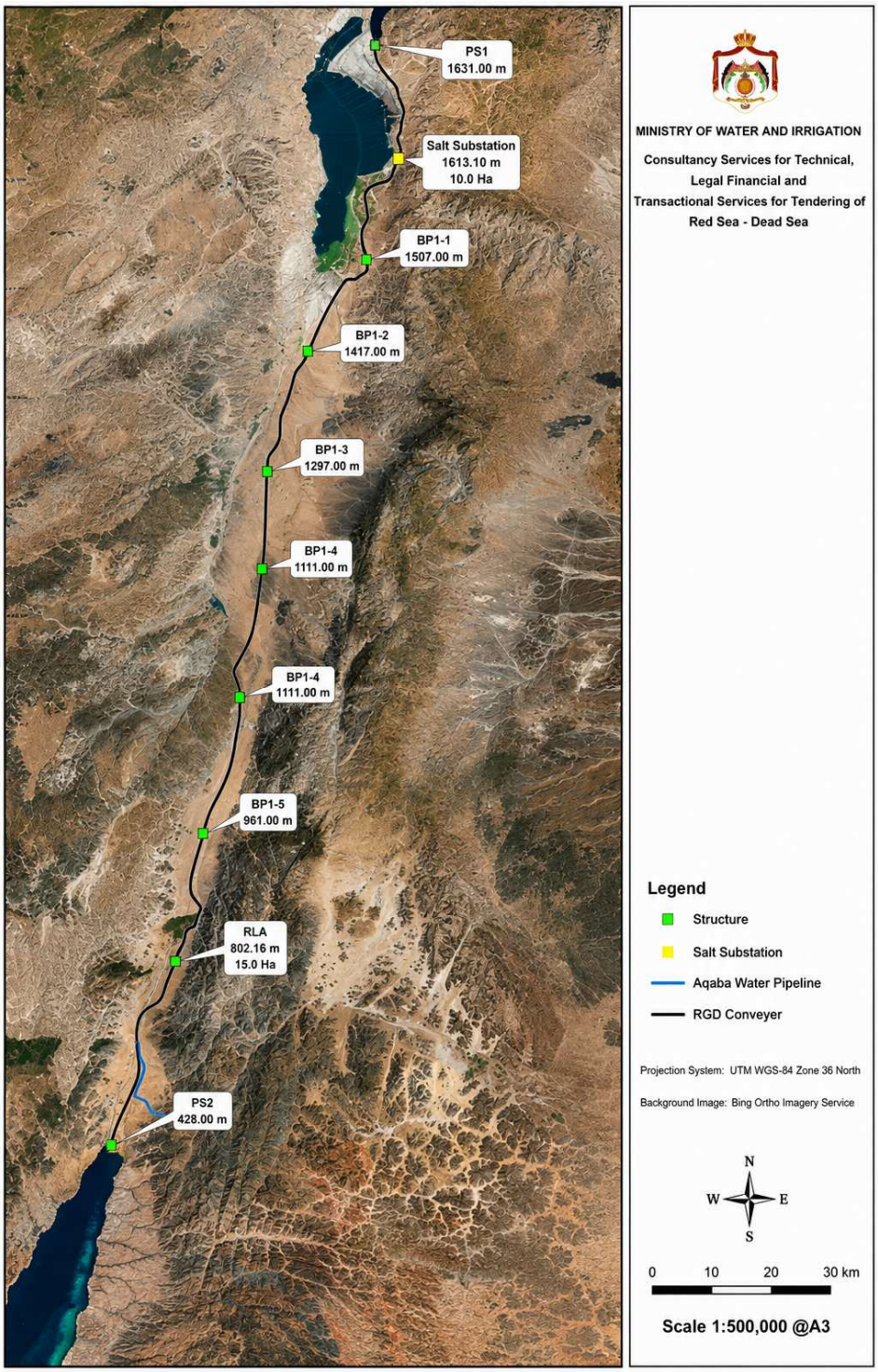

Fig. 26. Infrastructure of RSDS Project (Lazar et al., 2024)

Author Contributions: Conceptualization, B.S.K. and M.S.; methodology, A.E., B.S.K. and M.S.; software, A.E. and M.S.; validation, T.B.J., F.O.H. and H.F.; formal analysis, A.E., M.S. and M.A.G.; investigation, A.E. and M.S.; resources, B.S.K.; data curation, A.E. and M.A.G.; writing, original draft preparation, A.E.; writing, review and editing, B.S.K., T.B.J. and F.O.H.; visualization, M.S. and M.A.G.; supervision, B.S.K.; project administration, B.S.K.; funding acquisition, B.S.K. All authors have read and agreed to the published version of the manuscript.

Data Availability Statement: The data used in this study are publicly available from the IEEE Xplore source referenced in this work, namely *Prediction of Dead Sea Water Levels and Red-Dead Sea Canal Compensation to Balance Sea Levels*, document no. 8486191, available at: https://ieeexplore.ieee.org/abstract/document/8486191

References

Al-Bakri, J. T., Aljarrah, A., & Al-Kilani, M. R. (2026). Modeling climate change impacts on crop water requirement and yield under irrigated and rainfed conditions in Jordan's Mediterranean Highlands. *Potato Research, 69*(2), 56.

Asad Ahmad, O. (2026). Heavy metal source identification in Shafa Badran using geographic information system and three-dimensional modelling. *Journal of Water and Land Development,* 186-195.

Al Hasanat, H. A., Hassanat, A. B., Alharasees, O., Tarawneh, A. S., Altarawneh, G. A., Alhasanat, L. A., & Begović, M. (2025). Interpretable machine learning for imbalanced pedestrian injury severity prediction in urban Jordan. *Journal of King Saud University–Engineering Sciences, 37*(7), 1-42.

Al-Makhadmah, I. M., Al Najdawi, B. M., & Al-Muala, I. M. (2020). Impact of psychological empowerment on the performance of employees in the four- and five-star hotel sector in the Dead Sea--Jordan tourist area. *GeoJournal of Tourism and Geosites*, *30*(2), 896–904.

Alqadi, K. A., & Kumar, L. (2014). Water policy in Jordan. *International Journal of Water Resources Development*, *30*(2), 322–334.

Asmar, B. N. (2003). The science and politics of the Dead Sea: Red Sea canal or pipeline. *The Journal of Environment & Development*, *12*(4), 325–339.

Baer, G., Gavrieli, I., Swaed, I., & Nof, R. N. (2024). Remote sensing of floodwater-induced subsurface halite dissolution in a salt karst system, with implications for landscape evolution: The western shores of the Dead Sea. *Remote Sensing*, *16*(17), 3294.

Bentor, Y. K. (1961). Some geochemical aspects of the Dead Sea and the question of its age. *Geochimica et Cosmochimica Acta*, *25*(4), 239–260.

Bzour, A., Valánszki, I., & Mumtaz, A. (2025). Contemporary cultural significance of the Lower Jordan River Basin: The intersection between Jordan River as an ecological political border and the cultural significance. In *Fábos Conference on Landscape and Greenway Planning*. University of Massachusetts Amherst.

Ghazleha, S. A., Kempe, S., Hartmann, J., & Jansen, N. (2010). Rapidly shrinking Dead Sea urgently needs infusion of 0.9 km³/a from planned Red-Sea channel: Implication for renewable energy and sustainable development. *Jordan Journal of Mechanical and Industrial Engineering*, *4*(1), 211–216.

Lazar, M., Cheng, L., & Basson, U. (2024). Combined geophysical methods in extreme environments, An example from the Dead Sea. *Remote Sensing*, *16*(11), 1978.

Lensky, N. G., Dvorkin, Y., Lyakhovsky, V., Gertman, I., & Gavrieli, I. (2005). Water, salt, and energy balances of the Dead Sea. *Water Resources Research*, *41*(12), W12418.

Ohio State University. (2015). *Dead Sea products*. https://u.osu.edu/deadseaproducts/2015/04/

Salameh, E., & El-Naser, H. (2008). Restoring the shrinking Dead Sea, The environmental imperative. In H. Hotzl, U. Trolp, & A. Al-Karablieh (Eds.), *Climatic changes and water resources in the Middle East and North Africa* (pp. 453–468). Springer.

Seeberg, P. (2024). Hydro-hegemony and the Gaza War. *Middle East Policy*, *31*(2), 33–46.

Shekar, P. R., & Mathew, A. (2024). Morphometric analysis of watersheds: A comprehensive review of data sources, quality, and geospatial techniques. *Watershed Ecology and the Environment*, *6*, 13–25.

Sommer, U., & Fassbender, F. (2024). Environmental peacebuilding: Moving beyond resolving violence-ridden conflicts to sustaining peace. *World Development*, *178*, 106555.

Wikipedia. (2023a). *Penstock*. https://en.wikipedia.org/wiki/Penstock

Wikipedia. (2023b). *Red Sea–Dead Sea Water Conveyance*. https://en.wikipedia.org/wiki/Red_Sea–Dead_Sea_Water_Conveyance

Yousef, M. (2025). The Dead Sea Continental Transform Fault System: Accommodating left-lateral movement between the African and Arabian plates. In *Seismotectonics of the East Mediterranean-Red Sea Region* (pp. 161–180). Springer Nature Switzerland.

Zawahri, N. A., & Weinthal, E. (2025). The politicization of water: How water fell hostage to Jordanian politics. In *World Scientific handbook of transboundary water management: Science, economics, policy and politics: Volume 3: The role of formal and informal institutions in managing transboundary basins* (pp. 179–198). World Scientific Publishing.

© 2026 by the authors; licensee Growing Science, Canada. This is an open access article distributed under the terms and conditions of the Creative Commons Attribution (CC-BY) license (http://creativecommons.org/licenses/by/4.0/).